Published in final edited form as:
Neurobiol Dis. 2007 March ; 25(3): 649–664.

Acute and Long-Term Effects of Botulinum Neurotoxin on the Function and Structure of Developing Extraocular Muscles

Scott A. Croes, **Larisa M. Baryshnikova**, **Soniya S. Kaluskar**, and **Christopher S. von Bartheld**
Department of Physiology & Cell Biology, University of Nevada School of Medicine, Reno, Nevada 89557

Abstract

Strabismus is a misalignment of the visual axes, due to an imbalance in extraocular muscle (EOM) function. Botulinum neurotoxin (BoNT) treatment can correct the misalignment with permanent therapeutic effects in infants, possibly because the toxin causes structural alterations in developing EOM. To determine whether BoNT indeed permanently weakens developing EOMs, we examined the chicken oculomotor system. Following injections of BoNT in hatchling chicks, we quantified physiological parameters (contractile force measurements) and morphological parameters (myofiber morphometry, innervation, quantitative transmission electron microscopy of mitochondria/fiber types). Treatment of developing EOM with BoNT caused acute reductions of muscle strength and mitochondrial densities, but minimal changes in muscle fiber diameter and neuromuscular junction structures. Contrary to expectations, contractile force was fully recovered by 3–4 months after treatment. Thus, permanent therapeutic effects of BoNT most likely do not cause permanent changes at the level of the peripheral effector organ, but rather involve central (CNS) adaptive responses.

Keywords

oculomotor; motor endplate; neuromuscular junction; eye muscle; contractile force; mitochondria; botulinum toxin; strabismus

INTRODUCTION

Strabismus is a misalignment of the visual axes, due to an imbalance in extraocular muscle (EOM) function. Precise muscle force regulation is required to align the eyes for coordination of functional and binocular vision. Failure to maintain proper visual alignment results in a condition known as strabismus. Strabismus is one of the most prevalent ophthalmic disorders, affecting nearly 5% of the human population (Magramm, 1992; Stidwill, 1997; Tychsen, 2005). Infantile (pediatric or congenital) strabismus begins during the first year of life (Tychsen, 2005). Early treatment of infantile strabismus is particularly important, because visual alignment is required for proper binocular vision development and stereopsis (Hubel and Wiesel, 1965; Ing, 1981; Fenstemaker et al., 2001; Kind et al., 2002). Eye misalignment during this critical period can disrupt binocular fusion and may lead to amblyopia (permanent loss of vision in one eye) through the neural mechanism of suppression (Birch et al., 1990).

Corresponding Author: Christopher S. von Bartheld, Department of Physiology and Cell Biology, Mailstop 352, University of Nevada School of Medicine, Reno, NV 89557 (USA), Phone: (775) 784-6022 or 784-4635, Fax: (775) 784-6903, Email address: chrisvb@physio.unr.edu.

In the early 1970's, Scott and colleagues pioneered the use of botulinum neurotoxin (BoNT) as an effective alternative to conventional strabismus surgery (Scott et al., 1973). Since this time, BoNT has been effectively used for eye realignment in children and adults, but its use has been limited due to its relatively short duration of action, which often necessitates reinjection or transition to incisional surgery (Scott, 1980; Lee et al., 1988; Biglan et al., 1989; Ing, 1993; Tejedor and Rodriguez, 2001). In contrast, the application of BoNT in the treatment of pediatric strabismus, particularly infantile esotropia, has demonstrated permanent therapeutic results, but the effectiveness is related to the age at which the treatment is performed. Administration before the critical age of 7 months resulted in the lowest recurrence of esodeviation, whereas treatment after the age of 8 months did not provide the expected "stable" outcome and required additional applications (Magoon, 1989; Campos et al., 2000; McNeer et al., 2000, 2003).

These results suggest that the toxin may have permanent muscle-weakening effects in developing EOM (Campos et al., 2000). However, it is also possible that the toxin-induced changes are transient and the lasting therapeutic effects may involve central adaptive responses that "self-adjust" to maintain the stable binocular state (Campos et al., 2000; Tychsen, 2005). Although about 300 million people worldwide would benefit from BoNT treatment for eye alignment during their first year of life, the principal mechanism of action of this therapy in the oculomotor system is unknown, and the physiological and structural effects of the toxin during the relevant early phase of EOM development have not been examined. While a primate model system would theoretically be optimal for this task, it is prohibitively expensive to use adequate numbers of monkeys necessary for conclusive statistical analyses (e.g., Spencer and McNeer, 1987; Spencer et al., 1992). Mice and other rodents, while less costly, have relatively small eyes and make it technically difficult to manipulate EOMs for contractile force measurements. To conclusively determine BoNT's effects during development, an additional model system is needed that is both cost-effective and provides an easily accessible EOM system that is similar to humans. Avian models are particularly well suited for this task because of their relatively large eyes, well developed eye muscles, accessibility during development, and an evolutionarily conserved extraocular motor system (Maier et al., 1972; Heaton and Wayne, 1983; Porter et al., 1995). Experiments utilizing chickens in developmental studies are faster and more cost-effective than comparable ones in mammals, allowing for sufficiently large "n" values. Although chickens are lateral-eyed animals, they are a valuable experimental model to obtain precise information on EOM force, in particular during critical periods of visual and oculomotor system development. Here we determined in a chicken animal model whether BoNT permanently alters structural and/or physiological parameters of developing EOMs. Our study, the first comprehensive functional and structural analysis of BoNT's long-term effects in the oculomotor system, indicates that the success of BoNT treatment does not involve long-term peripheral alterations at the level of the EOM.

MATERIALS AND METHODS

Materials

Fertilized White Leghorn chicken eggs were obtained from a local supplier (California Golden Eggs, Inc.) and incubated in a humidified force-draft incubator at 37–38°C. Date of hatching was designated posthatch day 0 (P0). A total of about 260 chickens were used for this study. Animals were housed in a brooder with controlled temperature (23–25°C) on a 12 hr light/dark cycle and were provided chicken feed and water ad libitum. Experimental procedures described in this study were approved by the Institutional Animal Care and Use Committee of the University of Nevada, Reno. Botulinum neurotoxin type A (BoNT; 150 kD) was supplied by List Biological Laboratories Inc. (Campbell, CA; Product 130A). Primary antibodies were monoclonal anti-neurofilament 200 and anti-neurofilament 68 from Sigma (St. Louis, MO),

and synaptic vesicle antibody SV2 (supernatant) from the Developmental Studies Hybridoma Bank (The University of Iowa, Department of Biological Sciences, Iowa City, IA). Biotinylated secondary antibody (horse anti-mouse) was from Vector Laboratories (Burlingame, CA). Tetramethylrhodamine-conjugated α-bungarotoxin (Rh-αBTX) and Alexa 488 were from Molecular Probes (Eugene, OR).

Botulinum Neurotoxin Preparation

Botulinum neurotoxin type A (BoNT) was diluted to a concentration of 2.0 ng/μl in sterile phosphate-buffered saline (PBS) containing bovine serum albumin (BSA, 1.0 mg/ml). The BSA was added to insure maximum recovery and to minimize nonspecific loss of toxin potency during handling. Aliquots were stored at −80°C until use. Reconstituted BoNT has previously been shown to maintain potency if refrozen or refrigerated for two weeks before use (Sloop et al., 1997). Similarly, we found no evidence of decreased potency of toxin preparations frozen for up to four months before use. Prior to administration, BoNT was thawed and diluted in sterile PBS to give a final injection dose of 0.25 ng or 0.50 ng in a volume of 10 μl.

Determination of Botulinum Neurotoxin Dose

The primary method of measurement for BoNT potency is based on units. A unit is defined as the amount of toxin that is lethal in 50% (LD_{50}) of female Swiss Webster mice (body mass ~20g) following intraperitoneal (IP) injection (Schantz and Johnson, 1992; Aoki, 2001; Kedlaya, 2004). Various commercial preparations of BoNT differ in their unit value: BOTOX ®, 0.05 ng/U (Allergan, Inc.); DYSPORT®, 0.025 ng/U (Ipsen, Inc.); Oculinum®, 0.25 ng/U. Disparity in potency and the lack of correlation between the recommended doses has led to considerable confusion. List Biological Laboratories Inc., supplier of BoNT used in this study, does not specify a unit value or LD_{50} for their product. To find the optimal dosage of BoNT for the present study, we used a regional chemodenervation assay modified from Pearce et al., (1995). At day of hatching (P0), increasing doses of toxin (0.125–3.0 ng) were injected into and above the superior oblique muscle (see Injection Procedure, below). Four to five chicks were injected for each dose. Muscle paralysis was assessed, based on isometric twitch tension measurements (see Stimulation Parameters, below), and the remaining force at 2 and 7 days post-injection (Fig. 1). Time duration was based on a previous study showing that both DYSPORT® and BOTOX® reached their maximal effect of muscle paralysis within 2 to 3 days, respectively (Pearce et al., 1995). Toxin activity for a given preparation was assessed by evaluating the percent decrease in maximum isometric twitch tension for the superior oblique muscle.

Injection Procedure

At day of hatching (P0) chicks were anesthetized with sodium pentobarbital (Nembutal, 50 mg/kg, intramuscular) as assessed by the absence of withdrawal to digit pinch. The head was fixed in a stereotaxic frame and secured with a beak clamp. Using aseptic techniques, a dose of either 0.25 ng or 0.50 ng of BoNT (total volume: 10 μl) was injected into and above the belly of the superior oblique muscle. The thinness of the superior oblique muscle at this early stage of development necessitated partial delivery of the toxin to the muscle's exterior. BoNT has previously been shown to penetrate through muscle fascia, but spread is reduced by approximately 20–25% (Shaari et al., 1991). The toxin was delivered slowly (over 10 seconds) to allow diffusion of the toxin into the muscle and minimize leakage into the orbit (Christiansen et al., 2003). Control injections were identical to experimental injections, using an equivalent volume of sterile PBS. Preparations of BoNT and PBS were administered using disposable insulin syringes (28G1/2, Becton Dickinson, NJ), which have been shown to reliably eject volumes of 2–10 μl (von Bartheld, 1998). Chicks were monitored daily for inflammatory orbital discharge or evidence of discomfort.

Contractile Force Measurements

Extraocular muscle function was evaluated in situ with nerve and blood supply intact. Chicks were deeply anesthetized as described previously. Supplemental doses of sodium pentobarbital (50 mg/kg) were given intramuscularly to maintain depth of anesthesia. Body temperature was maintained between 37° and 39° C using a heat lamp. The animal was placed on its side and the head was immobilized with a stereotaxic frame. To maintain tissue moisture, Krebs buffer (38°C) was continuously supplied to the orbit during the muscle/nerve preparation and throughout the contractile experiment, unless otherwise stated. Krebs buffer contained the following (in mM): NaCl 120.4, KCl 5.9, $NaHCO_3$ 15.5, Glucose 11.5, $MgCl_2$ 1.2, NaH_2PO_4 1.2, $CaCl_2$ 2.5.

For each contraction experiment one superior oblique muscle (right side) was used per animal. The distal end of the superior oblique muscle was exposed by removal of the upper eyelid, superior portions of the conjunctiva/Tenons capsule, and nictitating membrane. Visible surface vessels were cauterized. Resting muscle length (L_R) was measured in situ by placing a 6–0 silk suture along the length of the muscle. The insertional tendon of the superior oblique muscle was isolated, tied with a 6–0 silk suture, and cut from the sclera. This suture was later used to attach the tendon to the force transducer. To partially deflate the eyeball, a small incision (~1 cm) was made through the cornea and the lens, aqueous humor and a portion of the vitreous humor was drained. A suture was tied to the sclera near the insertion of the superior rectus muscle and the eyeball was carefully pulled downward to expose the trochlear nerve and superior oblique muscle. The trochlear (IV) nerve was carefully trimmed of connective tissue near its entrance to the superior oblique muscle. The suture attached to the tendon of the superior oblique muscle was then tied to a calibrated 10 g isometric force transducer (World Precision Instruments, Sarasota, FL), resonance frequency of 300 Hz, that was secured on a micromanipulator (Narachige, East Meadow, NY). The force transducer arm was positioned (via x-, y-, and z-axis micromanipulation) with the line of force perpendicular to the animal's midline and elevated slightly above the horizontal plane of the animal's head (Christiansen et al., 2003). The configuration of the muscle, suture, and force transducer was adapted to approximate the natural pulling direction of the superior oblique muscle and to yield the maximal contraction force during stimulation as indicated by our preliminary tests. The in situ approach yields higher (and more valid) contractile forces than in vitro measurements (Chen and von Bartheld, 2004), and the obtained values are within a similar range previously reported for adult pigeon EOMs (Stelling and McVean, 1988).

Stimulation Parameters

In situ muscle force of the superior oblique muscle was measured in response to trochlear (IV) nerve stimulation at supramaximal intensities. Parallel platinum electrodes (0.3 mm tip diameter, 2 mm between poles) were positioned within the orbital cavity so that both electrodes made contact with the medial side of the trochlear nerve ~ 5 mm proximal to its entry into the superior oblique muscle. To ensure that evoked muscle stimulation occurred only through the nerve, Krebs buffer was removed before each stimulus was applied. Optimal muscle length (L_o) and supramaximal stimulation voltage (~15 V) were determined from micromanipulations of muscle length and a series of twitch contractions (1 Hz square-wave pulse, 0.2 ms duration) until twitch tension was maximal - maximum isometric twitch force (P_t). Three single-twitch contractions were delivered in 5 s intervals to determine the average P_t and twitch contraction time (ct) (onset of force to peak force). In situ L_o was determined by placing a 6–0 silk suture along the length of the muscle from its origin to where the insertional tendon was tied. The isometric twitch measurements were made prior to tetanic stimulation to avoid potentiation.

Maximum tetanic tension (P_o) was evaluated with a pulse duration of 0.2 ms, train duration of 200 ms, and stimulation rates in the range of 100–600 Hz (50 Hz increments). Each stimulation

train was separated by a 5 second interval to ensure a return to baseline force. The parameters of voltage and optimal length established for maximal isometric twitch were used for maximal tetanic tension measurements. It has been shown that whole-muscle tetanic tensions are obtained at the same muscle lengths as maximal isometric twitch tensions (Barmack et al., 1971). The maximum tetanic tension was seen at or near the fusion frequency of the muscle. Fusion frequency was defined as the stimulation frequency at which individual twitches could not be differentiated at the tension plateau (Goldberg et al., 1998). Fatigability was measured by a stimulation of 5 second duration at fusion frequency (Asmussen, 1978; Stelling and McVean, 1988). Fatigue resistance of the muscle was measured by taking the residual tension at the end of stimulation expressed as a percentage of the peak tension. Trochlear nerve stimulation was induced via a Grass S48 stimulator (Quincy, MA). Single-twitch and tetanic tension were measured with a data-acquisition system (Digidata 1322A; Axon Instruments, Union City, CA). At the conclusion of contractile measurements the attachment suture was cut, the muscle was dissected free from its origin, trimmed of nonmuscle tissue, blotted on filter paper, and the mass was determined on a Sartorius analytical balance (Sartorius BP 110S, Germany). Current tracings were exported to CorelDraw (version 12, Corel Corporation, Ottawa, Ontario, Canada) for processing of the figures.

Morphometry of Muscle Fibers

BoNT-treated and control superior oblique muscles were processed for morphometric analysis of myofiber diameters. Muscles were fixed in Methacarn (methanol, chloroform and acetic acid at volume ratios of 6:3:1), washed in methanol, cleared in xylene, and embedded in paraffin (Paraplast Plus; Oxford Labware, St. Louis, MO). Serial cross sections (10 μm thick) were taken at the mid-belly of each muscle and collected on Surgipath slides (Snowcoat X-tra; Surgipath, Richmond, IL). Slides were baked overnight at 40–45 °C. Sections were deparaffinized, stained with thionin, dehydrated in a graded ethanol series, and coverslipped with di-*n*-butyl-phthalate-xylene (DPX; BDH Laboratory Supplies, Poole, UK). Utilizing an upright microscope (Nikon Eclipse E 600) equipped with Nomarski optics, the muscle fibers were examined with 40X objectives. Extraocular muscles consist of two distinct regions that can be distinguished based on myofiber size and location. The outer orbital layer consists of relatively small diameter myofibers and lies adjacent to the periorbital bones whereas the inner global layer contains relatively larger fibers and lies adjacent to the eyeball (Porter et al., 1995). Cross sections of muscle fibers (30–50) from both orbital and global layers were randomly chosen and measured for diameter and area, blind as to treatment. Diameter and area were calculated using Simple PCI software (Thousand Oaks, CA).

Electron Microscopy and Mitochondrial Analysis

Animals were anesthetized by intramuscular injection with Nembutal (100 mg/kg body weight) and the extraocular muscles were dissected out and fixed in 2% paraformaldehyde and 1.5% glutaraldehyde in 0.1 M sodium cacodylate buffer (pH 7.4) for 3 hours. A total of 27 muscles were examined, 9 at 2 weeks, 6 at 11 weeks, and 12 at 16 weeks. The muscles were post-fixed in 1% osmium tetroxide for 1 hour. Tissues were dehydrated in a series of graded ethanols and propylene oxide, embedded in Spurr's resin, and polymerized at 60°C overnight. The center 1/3 of the muscle was sectioned in the transverse plane at three levels. Semithin sections (1 μm) were prepared and stained with 1% toluidine blue for orientation and monitoring of tissue quality, followed by preparation of ultrathin sections (70–80 nm) for electron microscopy. Sections were stained with 2.5% aqueous lead citrate. Random sections of the orbital and global layer were examined and images captured at 10,500x in a Philips CM 10 transmission electron microscope equipped with a Gatan 792 BioScan digital imaging system. Muscles were examined for myofiber types (Baryshnikova and von Bartheld, in preparation, 2006), and the mitochondria were measured to determine average diameter, perimeter, total area, and fractional area, separately for the orbital and global muscle fibers and 4 myofiber types. Images

were analyzed by using Simple PCI software (Thousand Oaks, CA). A total of 100 random images, from 30–60 orbital layer and 30–60 global-layer myofibers, for each condition (experimental or control), each with an area of 94.48 μm^2, were analyzed at a final magnification of 25,000x–35,000x for distribution and size of mitochondria. Samples from at least three chickens were used for analysis of each condition.

Neuromuscular Junction Morphometry

Similar to mammalian EOMs, the chick superior oblique muscle contained both en plaque and en grappe motor endplates. En plaque motor endplates are innervated by a single axon, use a twitch mode of contraction, and are characteristic of the typical motor endplate found in mature skeletal muscle (Porter et al., 1996). En grappe motor endplates can be singly or polyneuronally innervated, use a non-twitch or tonic mode of contraction, and are located at multiple sites along the length of an EOM fiber (Oda, 1986; Porter et al., 1996). The larger more compact en plaque endplates were easily distinguished from the en grappe endings, which appeared as small clusters of beads (each 2–5 μm in length) scattered along the muscle fibers. It was impossible to always differentiate the en grappe endings from background fluorescence. For these reasons, the morphological analysis was restricted to the larger, more compact, and clearly identifiable en plaque receptors (Croes and von Bartheld, 2005). Morphological measurements were assessed only for endplates that were on the top surface of the fiber with their borders clearly distinguishable.

Utilizing an upright fluorescent microscope (Nicon Eclipse E 600), sprout number was determined with a 60x oil immersion lens. The number of sprouts per axon terminal was quantified within each muscle by randomly selecting at least 50 NMJs among the collected sections. Dual color images of endplates and NMJs were acquired with a laser scanning confocal microscope (Model 1024; Bio-Rad, Hercules, CA) using a 60x oil immersion objective with a constant pinhole setting to preserve the thickness of the confocal plane. For dual color imaging, Rh-αBTX and green-fluorescence-conjugated secondary antibody labels were excited sequentially using the 568-nm and the 488-nm excitation lines of the krypton/argon laser. The laser intensity and gain settings were adjusted on a per-image basis. Full frame 1024 x 1024 pixel images of endplates and nerve terminals were collected. Data for endplate length and area was calculated using Simple PCI software (Thousand Oaks, CA).

Immunohistochemistry—To control for any changes that may have been induced by the physiological manipulations during the contraction experiments, a separate group of chickens was used exclusively for visualization and quantification of neuromuscular junction structures. At time of sacrifice, chickens were anesthetized by intracardial injection with sodium pentobarbital (Nembutal, 100 mg/kg) and perfused transcardially with 2% paraformaldehyde in phosphate-buffered saline (PBS). The superior oblique muscle was carefully dissected out, cryoprotected in 30% sucrose in PBS overnight, embedded in optimal cutting temperature (OCT) compound, and stored at –20 °C. It should be noted that muscle samples were not post-fixed. Many protocols call for this step, but we found superior antibody labeling when postfixing of samples was omitted (Croes and von Bartheld, 2005). Serial longitudinal sections (100 μm thick), parallel to the orientation of the muscle fibers, were cut on a cryotome (Leica CM 3050) and every 5^{th} section was collected. Sections were mounted on Surgipath micro slides (Snowcoat Xtra; Surgipath, Richmond, IL). Frozen sections were air dried for ~45 minutes, hydrated for 15 minutes with PBS and then treated with 10% bovine serum albumin (BSA) and 0.3% Triton X-100 for 1 hour. Anti-neurofilament antibodies (anti-neurofilament 68 and 200) were diluted 1:200 and synaptic vesicle antibody supernatant (SV2) was diluted 1:10, both with PBS. Sections were incubated for 24 hrs with primary antibodies and then washed with PBS (3 times/30 min each). The appropriate biotinylated secondary antibody was applied for 1 hour and washed (3 times/30 min each). Fluorophore, Alexa 488 (Molecular

Probes), was applied for 1 hour and washed (3 times/30 min each). Tetramethylrhodamine-conjugated α-bungarotoxin (Rh-αBTX) was applied for 45 minutes at a concentration of 2 μg/ml. Sections were washed and coverslipped with Aqua-mount (Lerner laboratories, Pittsburgh, PA) and stored in the dark at 4 °C until analysis.

Statistical Analysis

All statistical analyses were conducted using SigmaStat software (Jandel Corp, San Rafael, CA). The data are reported as the mean ± standard error of the mean. Statistical significance was evaluated by Student's paired t-test or one-way analysis of variance (ANOVA). For statistical significance, we used a confidence level of $p < 0.05$.

RESULTS

Determination of Botulinum Neurotoxin Dose

To measure the potency of BoNT that was purchased from List Biological Laboratories, we performed a chemodenervation assay of the superior oblique muscle. Regional chemodenervation is responsible for the therapeutic effect observed following intramuscular administration of botulinum toxin and thus potency of the toxin is more accurately predicted by directly measuring regional denervation rather than lethality (Pearce et al., 1995). Following a single injection of toxin (0.125 to 3.0 ng) into and above the belly of the superior oblique muscle, maximal isometric twitch tension was measured to determine the extent of muscle paralysis. The effectiveness of BoNT doses on twitch tension was measured after 2 and 7 days as compared to controls (saline injected), as shown in Figure 1. The amount of toxin used clinically in the treatment of strabismus is not intended to completely paralyze the overacting EOM. Thus, we sought a dose that would significantly reduce muscle strength without complete paralysis. The two largest doses tested (2.0 and 3.0 ng) reduced twitch tension by at least 97% for 7 days, which was considered too severe for the purposes of this study. A dosage of 0.50 ng of BoNT was selected for our investigation because this amount reduced twitch tension between 80% and 95% of controls, for at least 7 days. This dose elicited a significant decrease in muscle strength without complete paralysis. To evaluate whether developing EOMs exhibit a dose-dependent response to the toxin, 0.25 ng (1/2 the selected dose of 0.5 ng) of BoNT was also applied, which decreased muscle strength between 70% and 85% of controls, for at least 7 days.

Contractile Force Generation

BoNT induced dramatic force reductions in EOMs of adult cats within an 18 hour period (Dimitrova et al., 2002), but to our knowledge, the short and long-term effects of BoNT on the strength of developing EOM have not been investigated. In order to evaluate EOM force in response to the toxin we developed an in situ method (Croes and von Bartheld, 2006, in preparation) for stimulating the superior oblique muscle via the trochlear nerve. This method enabled us to effectively measure the contractile forces generated by the superior oblique muscle of chickens from hatchling to adult (Fig. 2 and 3).

Twitch tension—BoNT, at a dose of either 0.25 ng (low dose) or 0.5 ng (high dose), temporarily decreased the maximum force produced in response to a single-pulse or a train of pulses. Examples of twitch-tension recordings of control and BoNT treated animals at post-hatch day 7 and P28 are illustrated in Fig. 2A and B, respectively. At both the low and high dosages, twitch tension was significantly reduced from P2 to P42 ($p<0.05$). Single twitch was decreased to 14% (low dose) and 10% (high dose) of the control at 2 days post injection but recovered to 88% (low dose) and 85% (high dose) of control by P42. Twitch response returned to control values by P56 for the lower dose animals and by P112 for the higher dose animals as shown in Fig. 2C ($p<0.05$). Effects on contraction time are described below (Fig 2D).

Tetanic tension—BoNT administration had a similar transient effect on tetanic tension as seen in muscle twitch tension. Examples of tetanic tension recordings of control and BoNT treated animals at post-hatch day 7 and day 28 are illustrated in Fig. 3A and B, respectively. Tetanic tension was significantly reduced from P2 to P28 for both doses of toxin used. Tetanic tension was significantly decreased to 49% (low dose) and 23% (high dose) of control at 2 days post-injection and then gradually recovered to control levels by P42 for the lower dose animals and by P77 for the higher dose animals as shown in Fig. 3C ($P<0.05$). The earlier recovery of twitch and tetanic tension for the lower dose treatment groups indicates that the effects of BoNT on developing EOM are dose dependent. Fusion frequency for control animals was usually between 300 – 400 Hz. Fusion frequency is the stimulation frequency at which individual twitches could not be differentiated at the tension plateau (Goldberg et al., 1998). Maximum tetanic tension was reached at or close to the fusion frequency and further increases of the rate of stimulation did not lead to an increase in the developed tension.

Contraction time—Temporal characteristics of the twitch response were substantially affected after the application of BoNT (Fig. 2D). Twitch contraction time (onset of force to peak force) was significantly increased – yielding a slower contraction, from P2 until P28 to P42 of age, depending on the dose of toxin administered as shown in Fig 2D ($P<0.05$). At P2, contraction time was 9.71ms (± 0.20 ms, SEM) for controls, 12.71ms (± 0.70 ms) for low dose, and 13.47 ms (± 0.80 ms) for high dose treatment groups. By P28, the contraction time of the low dose animals was indistinguishable from controls, whereas the contraction time of the high dose animals remained significantly slower until age P42. From a developmental stand point it is interesting to note that the contraction time quickly (within two weeks) decreases as the superior oblique muscle matures. For example, twitch contraction time of control animals decreased from 9.71 ms (± 0.23 ms, SEM) at age P2 to 5.5 ms (± 0.20 ms) at age P14. Between P28 and P112, contraction time stabilized in control animals with values of 5.39 ms (± 0.12 ms) at P28 and 5.30 ms (± 0.10ms) at P112.

Fatigue—BoNT exposure did not cause an increase in fatigability of the superior oblique muscle at P112. After the muscle had been stimulated for 5 seconds at fusion frequency, the residual tension of the BoNT exposed animals was 32.42% (± 2.00%), while that of controls was 33.65% (± 1.64%). Since mitochondrial fractional area for the type II fibers within the orbital layer was still impaired in some regions (see Mitochondrial Ultrastructure and Distribution, below), we used muscle fatigue measurements as an indirect indication of muscle metabolic capacity and mitochondrial activity of the older animals (P112). We conclude that the reduced mitochondrial fractional area does not significantly alter the ability of the muscle to resist fatigue.

Taken together, the recovery of muscle function based on four commonly used physiological parameters (twitch and tetanic tension, fatigability, contraction time) indicates that these four major functional aspects of developing EOMs are not permanently altered by the toxin.

Myofiber Morphology

Extraocular muscles consist of two layers: an inner (central) global layer (GL) adjacent to the eyeball, and an outer (peripheral) orbital layer (OL) adjacent to the bones of the orbit (Spencer and Porter, 1988). The OL is narrow and consists of relatively small myofibers, whereas the GL is wider and contains larger myofibers (Kranjc et al., 2001). Depending on the method of classification, EOMs contain six to eight distinct fiber types differentially located within these layers and they are either multiply innervated (slow tonic contracting) en grappe fibers or singly innervated (fast contracting) en plaque fibers (Mayr, 1971; Porter and Baker, 1996; Wasicky et al., 2000). For adult EOM, there is some consensus that BoNT specifically affects the morphology of myofibers within the orbital layer and does not significantly alter the size of

myofibers within the global layer (Spencer and McNeer, 1987; Ohtsuki et al., 1998, Stahl et al., 1998; Kranjc et al., 2001). However, for developing EOM, little is known about the effects of BoNT on myofiber morphology. Thus, we quantified changes in myofiber diameter in both the orbital and global regions to document the toxin's effects on EOM development. Representative images of control and toxin-exposed EOM with distinct orbital and global layers are shown in Fig. 4A and B. There was a progressive rate of myofiber growth (diameter) in both control and BoNT treatment groups from P2 through P112, as expected, at least in the controls, as the developing EOM (superior oblique) matured (Fig. 4C). During the acute phase of paralysis, there was no difference in size between BoNT-treated and control myofibers. However, at 42 days post-injection, there was a small, but significant reduction in myofiber size in both the global and orbital layers as compared to control muscle. Muscle fiber diameters became significantly smaller in the global layer at P42 ($P<0.05$) with a mean diameter of 21.12 μm ± 0.73 μm versus 23.9 μm ± 0.80 μm in the control global layer muscle fibers. Similarly, orbital layer muscle fiber diameters became significantly smaller at P56 ($P<0.05$) with a mean diameter of 12.72 μm ± 0.12 μm versus 14.31 μm ± 0.17 μm in the controls. However, the BoNT induced muscle atrophy seen in both the global and orbital layers was temporary. By P77 and P112, muscle fiber diameters of BoNT treated superior oblique muscles were not significantly different from those of control values ($p>0.05$) (Fig. 4C). Thus, we can rule out reduction of myofiber size as a cause for the permanent therapeutic effect of BoNT treatment.

Mitochondrial Ultrastructure and Distribution

Mitochondria are sensitive markers for the functional state of muscles (Capetanaki, 2002; Drew and Leeuwenburgh, 2004; Fluck and Hoppeler, 2003; Hoppeler et al., 1987). Mitochondria respond to BoNT treatment in adult mammalian extraocular muscles with significant morphological alterations (Spencer and McNeer, 1987). As in mammals (Wasicky et al., 2000), up to four different muscle fiber types can be distinguished at the ultrastructural level in both the orbital and the global muscle fiber layer of chicken EOMs (Baryshnikova and von Bartheld, in preparation, 2006). To determine mitochondrial changes as a possible cause for long-term effects of BoNT, we examined sizes and the spatial distribution of mitochondria in superior oblique extraocular muscles from age-matched control chickens and chickens at 14, 77, 112, and 154 days after BoNT injections. Data for up to four myofiber types were analyzed separately. The typical appearance of mitochondria in developing avian EOMs is shown in Fig. 5A, C.

In the 2-week old chicks (P14), the size and distribution of mitochondria changed dramatically after treatment with BoNT, as we expected based on previous work in other species (Spencer et al., 1992; Ohtsuki et al., 1998). The average area, diameter, and perimeter of mitochondria in orbital and global muscle fibers of types I, II, and IV was significantly decreased (to 30–55%, Table 1). The average area, diameter and perimeter of larger mitochondria, in orbital muscle fibers of type III, were less dramatically decreased (to 67–81%, Table 2). The average area, diameter and perimeter of mitochondria in global muscle fibers of type III were also significantly decreased (to 35–67%, Table 2). Statistical analyses of mitochondrial size show that the differences between control and BoNT treatment groups for all parameters were statistically significant ($p\leq0.001$). The fractional area of mitochondria decreased in both orbital and global muscle fibers (Table 3). This effect was most evident in the complete loss of clusters of mitochondria in the subsarcolemmal region (Fig. 5B, Table 3). For this reason, the fractional area of mitochondria was assessed separately for the subsarcolemmal and the intermyofibrillar region (Table 3). In the acute phase of BoNT poisoning, the clustering of mitochondria was reduced as well as their average size.

In the 11-week old chickens (P77), some morphological parameters, in particular those of myofibers types I, II and IV in the global layer, had already fully recovered after BoNT

treatment (Table 1). However, the area and diameter of mitochondria was still reduced in the orbital layer for myofiber types I, II and IV (Table 2), and the perimeter of mitochondria was still abnormally low for myofiber type III (Table 2), and only the area and diameter of mitochondria had fully recovered in the orbital layer for myofiber type III (Table 2). Likewise, the fractional area was still abnormally low for several fiber types at 11 weeks, including the subsarcolemmal clusters in fiber type I in both the orbital and global layers (Table 3), as well as fiber type IV in the global layer (Table 3). Thus, some residual, statistically significant, morphological abnormalities persisted at 11 weeks after BoNT treatment.

In the 16-week old chickens (P112), the distribution and size of mitochondria was essentially fully recovered after treatment with BoNT (Fig. 5D). The morphometric data for mitochondria was not significantly different in either orbital or global muscle fibers (Tables 1–3), with one exception for the fractional area of mitochondria in the intermyofibrillar area of fiber type II in the orbital layer (Table 3). All other parameters (33 out of 34 that were measured for the different fiber types, including area, diameter, perimeter and fractional area) were statistically indistinguishable between the BoNT-treated and the control muscles.

In the 22-week old chickens (P154), the distribution, size and fractional area of mitochondria were statistically indistinguishable for all parameters between the BoNT-treated and the control muscles.

We attempted to also quantify the relative frequency of the four different muscle fiber types as a function of age and BoNT treatment, but realized that the frequencies varied too much with the sectioning plane as well as regional differences, and we concluded that, in contrast to mitochondrial morphology and distribution, overall or relative myofiber classification would thus be an unreliable indicator of BoNT effects.

Taken together, our data show that by quantitative morphological criteria of mitochondria, all the BoNT-treated orbital and global muscle fibers fully recovered between 11 and 22 weeks.

Motor Endplate Morphology

Chick EOMs contain both the larger en plaque and smaller en grappe motor endplates (Croes and von Bartheld, 2005), similar to what has been described in human EOM (Oda, 1986; Oda and Hiroshi, 1988; Spencer and Porter, 1988). Here we examined only the en plaque endplates because it is technically impossible to reliably measure the size of en grappe endings. To assess the developmental effect of BoNT (dose: 0.5 ng) on motor endplate size, we analyzed endplate morphology (area) in the superior oblique muscle from post-hatch day 2 (P2) through P112 (Fig. 5). Examination of the motor endplates showed a developmental change in acetylcholine receptor (AChR) cluster distribution (Fig. 6A) that appears to be a progression of what has been observed during embryonic development. As previously described for the embryonic period of development (between embryonic day 14 and P2 (Croes and von Bartheld, 2005), the AChRs that were initially clustered in the shape of oval plaques with a relatively uniform density eventually became perforated and displayed a “pretzel-like” morphology similar to that described for the NMJs of skeletal muscles (Balice-Gordon et al., 1990; Balice-Gordon and Lichtman, 1993; Sanes and Lichtman, 1999; Marques et al., 2000). This “pretzel-like” appearance continued throughout the experimental time period of P2 through P112. As expected, in both control and BoNT treated animals there was a progressive increase in motor endplate area as the animals matured from P2 to P112 (Fig. 6B). Throughout the experimental time period examined there were no significant differences in motor endplate area between control and toxin-treated animals ($p>0.05$). In controls, motor endplate area increased from 79.62 μm^2 (± 1.67 μm^2) at P2, to 252.20 μm^2 (± 12.32 μm^2) at P112; for BoNT treated animals, motor endplate area increased from 78.23μm^2 ($\pm 0.62\mu m^2$) at P2, to 256.08 μm^2 (± 14.70

μm^2) at P112. Thus, we conclude that treatment with BoNT during early EOM development does not affect motor endplate structure of the original parent neuromuscular junctions.

Nerve Terminal Morphology

BoNT causes sprout formation at the nerve terminals of both mature extraocular and skeletal muscle (Brown et al., 1980; Porter et al., 1991; de Paiva et al., 1999). In order to determine if the toxin induces a similar response in developing EOM, we counted the number of terminal sprouts per neuromuscular junction (NMJ) within the superior oblique muscles of control and BoNT treated (0.5 ng) animals ranging in age from P2 through P112. Control animals rarely exhibited sprout formation (Fig. 7E). Seven days after the injection of BoNT, terminal sprouts appeared as thin filament outgrowths which extended beyond the original endplate border, but were relatively infrequent, with 0.09 ± 0.02 (SEM) sprouts per NMJ (Fig. 7E). Between P28 and P42 the sprouts appeared to be in contact with distinguishable patches of ACh receptors that resembled new motor endplates (Fig. 7B, D). Correspondingly, there was an increase in twitch and tetanic tension of the BoNT treated animals during this time period (Figs. 2C and 3C), supporting the notion that these sprouts contribute to nerve-induced muscle contractions. However, based on our experimental methods we can only speculate as to the functionality of these sprouts. By P42, the number of terminal sprouts per NMJ had increased to 0.41 (± 0.07) and then declined to 0.26 (± 0.07) by P112 (Fig. 7E). The decrease observed at P77 and P112 is likely due to sprout elimination as the original nerve terminals regain their function, which has previously been described in skeletal muscle (de Paiva et al., 1999). The direction of sprout growth was preferentially along the longitudinal axis of the muscle fibers. We found no evidence that BoNT caused degenerative changes in either the presynaptic or postsynaptic components of the original NMJ. Thus we conclude that the BoNT treatment does not cause permanent structural alterations in the NMJs and collectively, these data support the notion that synapses formed between sprouts and muscle fibers can, at least temporarily, play a role in the functional recovery of EOM paralyzed by BoNT.

DISCUSSION

The response of developing EOMs to BoNT is unique among skeletal muscle in that the toxin's long-term effects are generally thought to be permanent. This notion is largely based on the permanent therapeutic outcome in the treatment of infantile strabismus (Campos et al., 2000; McNeer et al., 2000). The reasons for such age-dependent results may involve two fundamentally distinct mechanisms: (1) permanent alterations of muscle force in the periphery or (2) central nervous system adaptive responses. BoNT inhibits the release of acetylcholine at the neuromuscular junction, resulting in the paralysis of all muscle fiber types. The long-term improvement of eye alignment seen after treatment of immature EOM is generally thought to be due to morphological alterations of a specific muscle fiber type (Porter et al., 1991; Spencer et al., 1992; Kranjc et al., 2001). However, until now, convincing physiological experiments to support this notion have not been reported. Our comprehensive long-term study of the effects of BoNT on developing EOMs in terms of muscle morphology, physiology, and functional recovery shows that the toxin-induced paralysis of developing EOMs is transient, and is followed by a full functional recovery. Thus, we challenge the notion of significant permanent structural changes in EOMs, and favor a "recalibration" or "reset" hypothesis involving central adaptive responses to realign the eyes.

Full functional recovery of contractile force

Because of the permanent therapeutic effects seen clinically, we expected BoNT to cause a permanent decrease in contractile force in developing EOM. However, for the contractile parameters of twitch tension, tetanic tension, contraction time, and muscle fatigue, we found that the toxin-induced effects were not permanent. Developing EOMs regain full functional

strength within 3–4 months after acute toxin exposure, similar to results in other skeletal muscle (Brin, 1997; Defazio et al., 2002; Calace et al., 2003; de Paiva et al., 1999). The parameters used in this study to assess contractile force are widely used for the assessment of muscle function (Stelling and McVean, 1988). Naturally, we cannot exclude the possibility that physiological parameters, not examined here, remained permanently impaired or that human eye muscles may respond to BoNT in an entirely different way than avian eye muscles.

The active-pulley hypothesis put forth by Demer and colleagues (2000) needs to be considered when assessing the effects of BoNT on EOM force and alignment. It has been previously shown that only the global layer of the rectus muscles inserts into the globe and that the orbital layer, constituting nearly half of the total fibers, inserts into a connective tissue pulley that encircles the globe near its equator in Tenon's fascia (Demer et al., 1997). The pulleys are suspended from the boney orbit by collagen/elastin/smooth muscle struts (Demer et al., 1995; Porter et al., 1996). The global fibers of each rectus muscle are responsible for rotating the eye, while the orbital fibers insert on their pulley to position the globe linearly and thus influence the EOM's rotational axis and prevent muscle sideslip during ocular rotations (Demer et al., 2000). If the orbital fibers of the superior oblique muscle also insert into a connective tissue pulley, then our contractile measurements would not have recorded the entire force generated by the orbital layer and we cannot conclude that contractile force returned for this muscle layer. However, since the BoNT-induced changes in both myofiber size and mitochondrial morphology/distribution are transient within both the global and orbital layer, it is reasonable to assume that the contractile strength of orbital fibers eventually returns to normal – like that of global fibers. Thus, based on an extensive series of data for four commonly used physiological parameters, we conclude that in our model system, major functional aspects are not permanently altered by the toxin and thus most likely cannot account for the lasting therapeutic effects seen in the treatment of infantile strabismus. To further assess the possibility of permanent effects we also examined structural changes at the level of the NMJ and myofiber mitochondria.

Endplate morphology and terminal sprouting was moderately affected by BoNT

BoNT inhibits the release of ACh from motor nerve terminals, resulting in muscle paralysis. The "typical" skeletal muscle response includes the development of nerve terminal sprouts that, in turn, stimulate the formation of new motor endplates (Duchen and Strich, 1968; Duchen, 1970; Porter et al., 1991; de Paiva et al., 1999). Over time, the functional recovery of the original neuromuscular junction (NMJ) results in the retraction of the terminal sprouts and disassembly of newly formed motor endplates (de Paiva et al., 1999). Similarly, BoNT exposure of EOMs results in the development of nerve terminal sprouts and the formation of new motor endplates but does not affect motor endplate size of the original NMJs.

BoNT exposure of limb skeletal muscle causes a trend toward larger motor endplates, but the overall size was not significantly different from that of controls (Bambrick and Gordon, 1987; Alderson et al., 1991; Witzemann et al., 1991; Ma et al., 2004). Similarly, our results of developing EOM indicate that BoNT induced a tendency, although not significant, for increased surface area of the motor endplates. The incorporation of new AChRs into the original motor endplate is thought to contribute to the recovery process in conjunction with nerve terminal sprouts that stimulate the formation of new motor endplates (Ma et al., 2004).

BoNT exposure of EOMs resulted in far fewer sprouts per NMJ than previously shown for other skeletal muscle (Holland and Brown, 1981; Angaut-Petit et al., 1990; Holds et al., 1990; de Paiva et al., 1999). For example, in the sternomastoid muscle of mice, the number of terminal sprouts increased to a maximum of ~4 sprouts per NMJ by 42 days after toxin exposure and then slowly decreased thereafter (de Paiva et al., 1999). In our developing EOM, sprout formation reached a maximum of only 0.41 sprouts per NMJ. The comparatively fewer sprouts

seen in our study would seem to indicate a relatively slow recovery, yet our contractile data demonstrate notable functional recovery within 4 weeks and complete recovery of muscle force within 4 months. This suggests that the functional recovery of our developing EOM was due primarily to the restoration of the original terminals in nerve-muscle transmission. Taken together, we conclude that there is no structural evidence for a permanent dysfunction of the NMJs.

Myofiber size was transiently affected by BoNT

In developing EOMs, BoNT induced a small, but statistically significant, late transient myofiber atrophy within both the global and orbital layers. Based on previous studies, the reduction of myofiber size seen within the orbital layer was expected. Prior investigations using adult EOM have shown that BoNT does not alter the size of all myofiber types equally, but instead tends to have its greatest morphological effect on the orbital, singly innervated muscle fibers (equivalent to our fiber type II) (Spencer and McNeer, 1987; Spencer et al., 1992; Ohtsuki et al., 1998; Kranjc et al., 2001). Such alterations in this particular fiber type have been postulated to play an important role in eye alignment during the treatment of strabismus (Porter et al., 1995). Our finding of a late transient reduction of myofiber size within the global layer was unexpected and appears to be unique to developing EOM. These data raise the possibility that the response to BoNT seen in developing EOM of human infants may involve myofibers of both the global as well as the orbital layers that contribute to the effectiveness seen clinically in the treatment of infantile strabismus. The transient atrophy of myofibers within both layers of developing EOM is more similar to the response of limb skeletal muscle where BoNT causes nonselective transient atrophy of virtually all muscle fibers (Duchen, 1970; Porter et al., 1991; Horn et al., 1993).

Effects on Mitochondria

Mitochondria are sensitive markers for the functional state of muscles (Capetanaki, 2002; Drew and Leeuwenburgh, 2004; Fluck and Hoppeler, 2003), and BoNT treatment in adult and juvenile mammalian EOMs has significant effects on mitochondria, particularly in the acute phase of paralysis (Spencer, 1987; Spencer et al., 1992). Therefore, we paid particular attention to the acute and long-term effects of BoNT treatment on quantitative and spatial aspects of mitochondria in developing chicken EOMs. With single BoNT doses that reduce muscle force to 10–20%, all of the quantitative mitochondrial parameters were reduced, but only transiently, and then fully recovered by 11–22 weeks after the toxin treatment. Full recovery included the orbital myofiber type II, which had previously been implicated in the long-term therapeutic effects of BoNT treatment (Porter et al., 1995). However, our measurements of contractile force clearly show that, at least with physiological parameters measured here, there was no lasting functional effect of the BoNT treatment. Therefore, the return of mitochondrial parameters back to normal in all 34 parameters that were assessed (Tables 1–3), together with the lack of any measurable permanent alterations in contractile force, indicates the lack of permanent structural changes in the developing EOMs, and thus the EOMs themselves are not likely responsible for the long-term therapeutic effects of BoNT.

Mechanisms of how BoNT may cause permanent change in eye alignment

Provided that the response of developing chick EOM to BoNT is similar to that of human infants, our results indicate that the transient reduction of twitch tension, tetanic tension, and contraction time cannot be responsible for the permanent therapeutic effect. Other mechanisms of sensory adaptation regulating oculomotor control likely contribute to maintain the therapeutic effects of early eye realignment. We postulate that the reason for the toxin's permanent effects seen clinically is predominantly due to the timing of the treatment and not to an enduring functional decrease of developing EOM strength. There is considerable evidence

for a critical period of binocular vision development and stereopsis within the cortex (Fenstemaker et al., 2001; Kind et al., 2002). If the eyes are properly aligned during this critical period of development, then the brain can "recalibrate" or "self-adjust" the oculomotor control system to generate the vergence error commands that guide eye alignment for binocular vision (Campos et al., 2000; Tychsen, 2005). The visual information may be used in the adaptive control of oculomotor subsystems so that during postparalytic muscle recovery, when ocular deviation might return, the new-found binocular state is maintained by corresponding reductions in oculomotor motoneuron output (i.e., gain) (Porter et al., 1991). Although BoNT does not alter the firing pattern of mature motor neurons (Moreno-Lopez et al., 1997), it is possible that such firing patterns could change after injection into the EOMs of younger animals (Dimitrova et al., 2002). Thus, even though the effect of the toxin on immature EOM is temporary, by the time the weakened muscle recovers and regains its strength, the brain circuits controlling eye alignment have been recalibrated and maintain the eyes in their proper alignment.

Acknowledgements

We thank Will Hatton for technical assistance in the use of the confocal microscope and Sean Ward for critical comments. The synaptic vesicle (SV2) antibody was obtained from the Developmental Studies Hybridoma Bank developed under the auspices of the NICHD and maintained by The University of Iowa, Department of Biological Sciences, Iowa City, IA 52242. Our work was supported by NIH grants EY 12841 and P20 RR 15581 from the National Center for Research Resources (NCRR).

Literature Cited

Asmussen G. The properties of the extraocular muscles of the frog. I. Mechanical properties of the isolated superior oblique and superior rectus muscles. Acta Biol. Med Ger 1978;37:301–312.

Alderson K, Holds JB, Anderson RL. Botulinum-induced alteration of nerve-muscle interactions in the human orbicularis oculi following treatment for blepharospasm. Neurology 1991;41:1800–1805. [PubMed: 1944912]

Angaut-Petit D, Molgo J, Comella JX, Faille L, Tabti N. Terminal sprouting in mouse neuromuscular junctions poisoned with botulinum type A toxin: morphological and electrophysiological features. Neuroscience 1990;37:799–808. [PubMed: 1701041]

Aoki KR. A comparison of the safety margins of botulinum neurotoxin serotypes A, B, and F in mice. Toxicon 2001;39:1815–1820. [PubMed: 11600142]

Balice-Gordon RJ, Lichtman JW. In vivo observations of pre- and postsynaptic changes during the transition from multiple to single innervation at developing neuromuscular junctions. J Neurosci 1993;13:834–855. [PubMed: 8426240]

Balice-Gordon RJ, Breedlove SM, Bernstein S, Lichtman JW. Neuromuscular junctions shrink and expand as muscle fiber size is manipulated: in vivo observations in the androgen-sensitive bulbocavernosus muscle of mice. J Neurosci 1990;10:2660–2671. [PubMed: 2388082]

Bambrick L, Gordon T. Acetylcholine receptors and sodium channels in denervated and botulinum-toxin-treated adult rat muscle. J Physiol 1987;382:69–86. [PubMed: 2442368]

Barmack NH, Bell CC, Rence BG. Tension and rate of tension development during isometric responses of extraocular muscle. J Neurophysiol 1971;34:1072–1079. [PubMed: 5115911]

Biglan AW, Burnstine RA, Rogers GL, Saunders RA. Management of strabismus with botulinum A toxin. Ophthalmology 1989;96:935–943. [PubMed: 2771360]

Birch EE, Stager DR, Berry P, Everett ME. Prospective assessment of acuity and stereopsis in amblyopic infantile esotropes following early surgery. Invest Ophthalmol Vis Sci 1990;31:758–765. [PubMed: 2335443]

Brin MF. Dosing, administration, and a treatment algorithm for use of botulinum toxin A for adult-onset spasticity. Spasticity Study Group. Muscle Nerve 1997;6:208–220.

Brin MF, Blitzer A. Botulinum toxin: dangerous terminology errors. J R Soc Med 1993;86:493–494. [PubMed: 8078064]

Brown MC, Holland RL, Ironton R. Nodal and terminal sprouting from motor nerves in fast and slow muscles of the mouse. J Physiol 1980;306:493–510. [PubMed: 7463373]

Calace P, Cortese G, Piscopo R, et al. Treatment of blepharospasm with botulinum neurotoxin type A: long-term results. Eur J Ophthalmol 2003;13:331–336. [PubMed: 12872788]

Campos EC, Schiavi C, Bellusci C. Critical age of botulinum toxin treatment in essential infantile esotropia. J Pediatr Ophthalmol Strabismus 2000;37:328–332. [PubMed: 11392405]

Capetanaki Y. Desmin cytoskeleton: a potential regulator of muscle mitochondrial behavior and function. Trends Cardiovasc Med 2002;12:339–348. [PubMed: 12536120]

Chen J, von Bartheld CS. Role of exogenous and endogenous trophic factors in the regulation of extraocular muscle strength during development. Invest Ophthalmol Vis Sci 2004;45:3538–3545. [PubMed: 15452060]

Christiansen SP, Becker BA, Iaizzo PA, McLoon LK. Extraocular muscle force generation after ricin-mAb35 injection: implications for strabismus treatment. J AAPOS 2003;7:1–6. [PubMed: 12690362]

Croes SA, von Bartheld CS. Development of the neuromuscular junction in extraocular muscles of white Leghorn chicks. Anat Rec A Discov Mol Cell Evol Biol 2005;282:110–119. [PubMed: 15627981]

de Paiva A, Meunier FA, Molgo J, Aoki KR, Dolly JO. Functional repair of motor endplates after botulinum neurotoxin type A poisoning: biphasic switch of synaptic activity between nerve sprouts and their parent terminals. Proc Natl Acad Sci USA 1999;96:3200–3205. [PubMed: 10077661]

Defazio G, Abbruzzese G, Girlanda P, et al. Botulinum toxin A treatment for primary hemifacial spasm: a 10-year multicenter study. Arch Neurol 2002;59:418–420. [PubMed: 11890846]

Demer JL, Miller JM, Poukens V, Vinters HV, Glasgow BJ. Evidence for fibromuscular pulleys of the recti extraocular muscles. Invest Ophthalmol Vis Sci 1995;36:1125–1136. [PubMed: 7730022]

Demer JL, Poukens V, Miller JM, Micevych P. Innervation of extraocular pulley smooth muscle in monkeys and humans. Invest Ophthalmol Vis Sci 1997;38:1774–1785. [PubMed: 9286266]

Demer JL, Oh SY, Poukens V. Evidence for active control of rectus extraocular muscle pulleys. Invest Ophthalmol Vis Sci 2000;41:1280–1290. [PubMed: 10798641]

Dimitrova DM, Shall MS, Goldberg SJ. Short-term effects of botulinum toxin on the lateral rectus muscle of cat. Exp Brain Res 2002;147:449–455. [PubMed: 12444476]

Drew B, Leeuwenburgh C. Ageing and subcellular distribution of mitochondria: role of mitochondrial DNA deletions and energy production. Acta Physiol Scand 2004;182:333–341. [PubMed: 15569094]

Duchen LW, Strich SJ. The effects of botulinum toxin on the pattern of innervation of skeletal muscle in the mouse. Q J Exp Physiol Cogn Med Sci 1968;53:84–89. [PubMed: 4297234]

Duchen LW. Changes in motor innervation and cholinesterase localization induced by botulinum toxin in skeletal muscle of the mouse: differences between fast and slow muscles. J Neurol Neurosurg Psychiatry 1970;33:40–54. [PubMed: 4907278]

Fenstemaker SB, Kiorpes L, Movshon JA. Effects of experimental strabismus on the architecture of macaque monkey striate cortex. J Comp Neurol 2001;438:300–317. [PubMed: 11550174]

Fluck M, Hoppeler H. Molecular basis of skeletal muscle plasticity - from gene to form and function. Rev Physiol Biochem Pharmacol 2003;146:159–216. [PubMed: 12605307]

Goldberg SJ, Meredith MA, Shall MS. Extraocular motor unit and whole-muscle responses in the lateral rectus muscle of the squirrel monkey. J Neurosci 1998;18:10629–10639. [PubMed: 9852598]

Heaton MB, Wayne DB. Patterns of extraocular innervation by the oculomotor complex in the chick. J Comp Neurol 1983;216:245–252. [PubMed: 6306064]

Holds JB, Alderson K, Fogg SG, Anderson RL. Motor nerve sprouting in human orbicularis muscle after botulinum A injection. Invest Ophthalmol Vis Sci 1990;31:964–967. [PubMed: 2335457]

Holland RL, Brown MC. Nerve growth in botulinum toxin poisoned muscles. Neuroscience 1981;6:1167–1179. [PubMed: 7279219]

Hoppeler H, Hudlicka O, Uhlmann E. Relationship between mitochondria and oxygen consumption in isolated cat muscles. J Physiol 1987;385:661–675. [PubMed: 3309266]

Horn AK, Porter JD, Evinger C. Botulinum toxin paralysis of the orbicularis oculi muscle. Types and time course of alterations in muscle structure, physiology and lid kinematics. Exp Brain Res 1993;96:39–53. [PubMed: 8243582]

Hubel DH, Wiesel TN. Binocular interaction in striate cortex of kittens reared with artificial squint. J Neurophysiol 1965;28:1041–1059. [PubMed: 5883731]

Ing MR. Early surgical alignment for congenital esotropia. Trans Am Ophthalmol Soc 1981;79:625–663. [PubMed: 7043869]

Ing MR. Botulinum alignment for congenital esotropia. Ophthalmology 1993;100:318–322. [PubMed: 8459999]

Kedlaya, D. Botulinum toxin: overview. 2004. eMedicine (cited 2004 Nov 15). Available from http://www.emedicine.com/pmr/topic216.htm

Kind PC, Mitchell DE, Ahmed B, Blakemore C, Bonhoeffer T, Sengpiel F. Correlated binocular activity guides recovery from monocular deprivation. Nature 2002;416:430–433. [PubMed: 11919632]

Kranjc BS, Sketelj J, D'Albis A, Erzen I. Long-term changes in myosin heavy chain composition after botulinum toxin a injection into rat medial rectus muscle. Invest Ophthalmol Vis Sci 2001;42:3158–3164. [PubMed: 11726617]

Lee J, Elston J, Vickers S, Powell C, Ketley J, Hogg C. Botulinum toxin therapy for squint. Eye 1988;2:24–28. [PubMed: 3410137]

Ma J, Elsaidi GA, Smith TL, Walker FO, Tan KH, Martin E, Koman LA, Smith BP. Time course of recovery of juvenile skeletal muscle after botulinum toxin A injection: an animal model study. Am J Phys Med Rehabil 2004;83:774–780. [PubMed: 15385786]

Magoon EH. Chemodenervation of strabismic children. A 2- to 5-year follow-up study compared with shorter follow-up. Ophthalmology 1989;96:931–934. [PubMed: 2771359]

Magramm I. Amblyopia: etiology, detection, and treatment. Pediatr Rev 1992;13:7–14. [PubMed: 1734442]

Maier A, Eldred E, Edgerton VR. Types of muscle fibers in the extraocular muscles of birds. Exp Eye Res 1972;13:255–265. [PubMed: 4260555]

Marques MJ, Conchello J-A, Lichtman JW. From plaque to pretzel: fold formation and acetylcholine receptor loss at the developing neuromuscular junction. J Neurosci 2000;20:3663–3675. [PubMed: 10804208]

Mayr R. Structure and distribution of fiber types in the external eye muscles of the rat. Tissue Cell 1971;3:433–462.

McLoon LK, Christiansen SP. Increasing extraocular muscle strength with insulin-like growth factor II. Invest Ophthalmol Vis Sci 2003;44:3866–3872. [PubMed: 12939302]

McNeer KW, Tucker MG, Spencer RF. Management of essential infantile esotropia with botulinum toxin A: review and recommendations. J Pediatr Ophthalmol Strabismus 2000;37:63–67. [PubMed: 10779262]

McNeer KW, Tucker MG, Guerry CH, Spencer RF. Incidence of stereopsis after treatment of infantile esotropia with botulinum toxin A. J Pediatr Ophthalmol Strabismus 2003;40:288–292. [PubMed: 14560837]

Moreno-Lopez B, de la Cruz RR, Pastor AM, Delgado-Garcia JM. Effects of botulinum neurotoxin type A on abducens motoneurons in the cat: alterations of the discharge pattern. Neuroscience 1997;81:437–455. [PubMed: 9300433]

Oda K. Motor innervation and acetylcholine receptor distribution of human extraocular muscle fibres. J Neurol Sci 1986;74:125–133. [PubMed: 3734834]

Oda K, Hiroshi S. Antigenic differences of acetylcholine receptor between single and multiple form endplates of human extraocular muscle. Brain Res 1988;449:337–340. [PubMed: 2456129]

Ohtsuki H, Hasebe S, Okano M, Furuse T. Morphological changes in the orbital surface layer muscle of the rabbit eye produced by botulinum toxin. Ophthalmologica 1998;212:53–60. [PubMed: 9438587]

Pearce LB, Borodic GE, Johnson EA, First ER, MacCallum RD. The median paralysis unit: A more pharmacologically relevant unit of biologic activity for botulinum toxin. Toxicon 1995;33:217–227. [PubMed: 7597725]

Porter JD, Strebeck S, Capra NF. Botulinum-induced changes in monkey eyelid muscle. Comparison with changes seen in extraocular muscle. Arch Ophthalmol 1991;109:396–404. [PubMed: 2003802]

Porter JD, Baker RS, Ragusa RJ, Brueckner JK. Extraocular muscles: basic and clinical aspects of structure and function. Surv Ophthalmol 1995;39:451–484. [PubMed: 7660301]

Porter JD, Poukens V, Baker RS, Demer JL. Structure-function correlations in the human medial rectus extraocular muscle pulleys. Invest Ophthalmol Vis Sci 1996;37:468–472. [PubMed: 8603853]

Porter JD, Baker RS. Muscles of a different 'color': the unusual properties of the extraocular muscles may predispose or protect them in neurogenic and myogenic disease. Neurology 1996;46:30–37. [PubMed: 8559415]

Sanes JR, Lichtman JW. Development of the vertebrate neuromuscular junction. Annu Rev Neurosci 1999;22:389–442. [PubMed: 10202544]

Schantz EJ, Johnson EA. Properties and use of botulinum toxin and other microbial neurotoxins in medicine. Microbiol Rev 1992;56:80–99. [PubMed: 1579114]

Scott AB, Rosenbaum A, Collins CC. Pharmacologic weakening of extraocular muscles. Invest Ophthalmol 1973;12:924–927. [PubMed: 4203467]

Scott AB. Botulinum toxin injection into extraocular muscles as an alternative to strabismus surgery. Ophthalmology 1980;87:1044–1049. [PubMed: 7243198]

Shaari CM, George E, Wu BL, Biller HF, Sanders I. Quantifying the spread of botulinum toxin through muscle fascia. Laryngoscope 1991;101:960–964. [PubMed: 1886444]

Sloop RR, Cole BA, Escutin RO. Reconstituted botulinum toxin type A does not lose potency in humans if it is refrozen or refrigerated for 2 weeks before use. Neurology 1997;48:249–253. [PubMed: 9008526]

Spencer RF, McNeer KW. Botulinum toxin paralysis of adult monkey extraocular muscle. Structural alterations in orbital, singly innervated muscle fibers. Arch Ophthalmol 1987;105:1703–1711. [PubMed: 3318773]

Spencer RF, Porter JD. Structural organization of the extraocular muscles. Rev Oculomot Res 1988;2:33–79. [PubMed: 3153651]

Spencer, RF.; Tucker, MG.; McNeer, KW.; Porter, JD. Experimental studies of pharmacological and surgical denervation of extraocular muscles in adult and infant monkeys. In: Scott, AB., editor. Trans Symposium “Mechanics of Strabismus”. San Francisco, Calif: 1992. p. 207-227.

Stahl JS, Averbuch-Heller L, Remler BF, Leigh RJ. Clinical evidence of extraocular muscle fiber-type specificity of botulinum toxin. Neurology 1998;51:1093–1099. [PubMed: 9781535]

Stelling J, McVean A. The contractile properties and movement dynamics of pigeon eye muscle. Pflugers Arch 1988;412:314–321. [PubMed: 3186434]

Stidwill D. Epidemiology of strabismus. Ophthalmic Physiol Opt 1997;17:536–539. [PubMed: 9666929]

Tejedor J, Rodriguez JM. Long-term outcome and predictor variables in the treatment of acquired esotropia with botulinum toxin. Invest Ophthalmol Vis Sci 2001;42:2542–2546. [PubMed: 11581195]

Tychsen, LF. Strabismus: the scientific basis. In: Taylor, DH.; Hoyt, Cs, editors. Chapter 76. Pediatric Ophthalmology and Strabismus. 3. Elsevier-Saunders; 2005.

von Bartheld CS. Radio-iodination of neurotrophins and their delivery in vivo: advantages of membrane filtration and the use of disposable syringes. J Neurosci Methods 1998;79:207–215. [PubMed: 9543487]

Wasicky R, Ziya-Ghazvini F, Blumer R, Lukas JR, Mayr R. Muscle fiber types of human extraocular muscles: a histochemical and immunohistochemical study. Invest Ophthalmol Vis Sci 2000;41:980–990. [PubMed: 10752931]

Witzemann V, Brenner HR, Sakmann B. Neural factors regulate AChR subunit mRNAs at rat neuromuscular synapses. J Cell Biol 1991;114:125–141. [PubMed: 1646821]

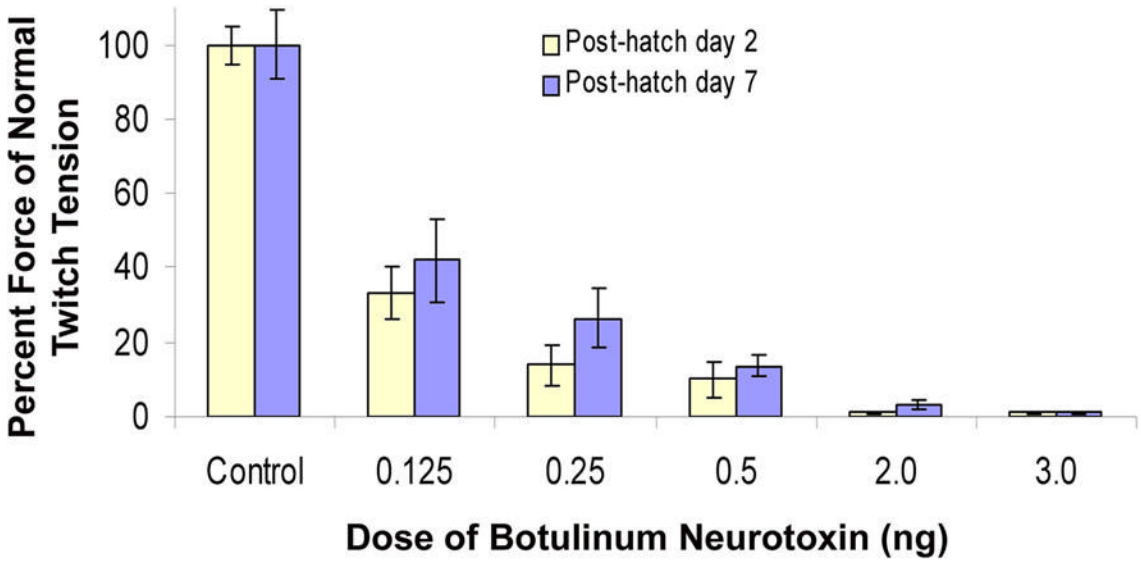

Figure 1.

Extent (severity) of extraocular muscle paralysis produced by increasing doses of botulinum neurotoxin (BoNT). On the day of hatching (P0), chicks were injected with a single dose of BoNT into and above the belly of the superior oblique muscle. The effect is shown as a function of dose and the percent of twitch tension is compared to controls (saline injected) for two time points: 2 days and 7 days after injection. For absolute values of force tension, see Fig. 2. Three to five chicks were used for each condition. Error bars = SEM.

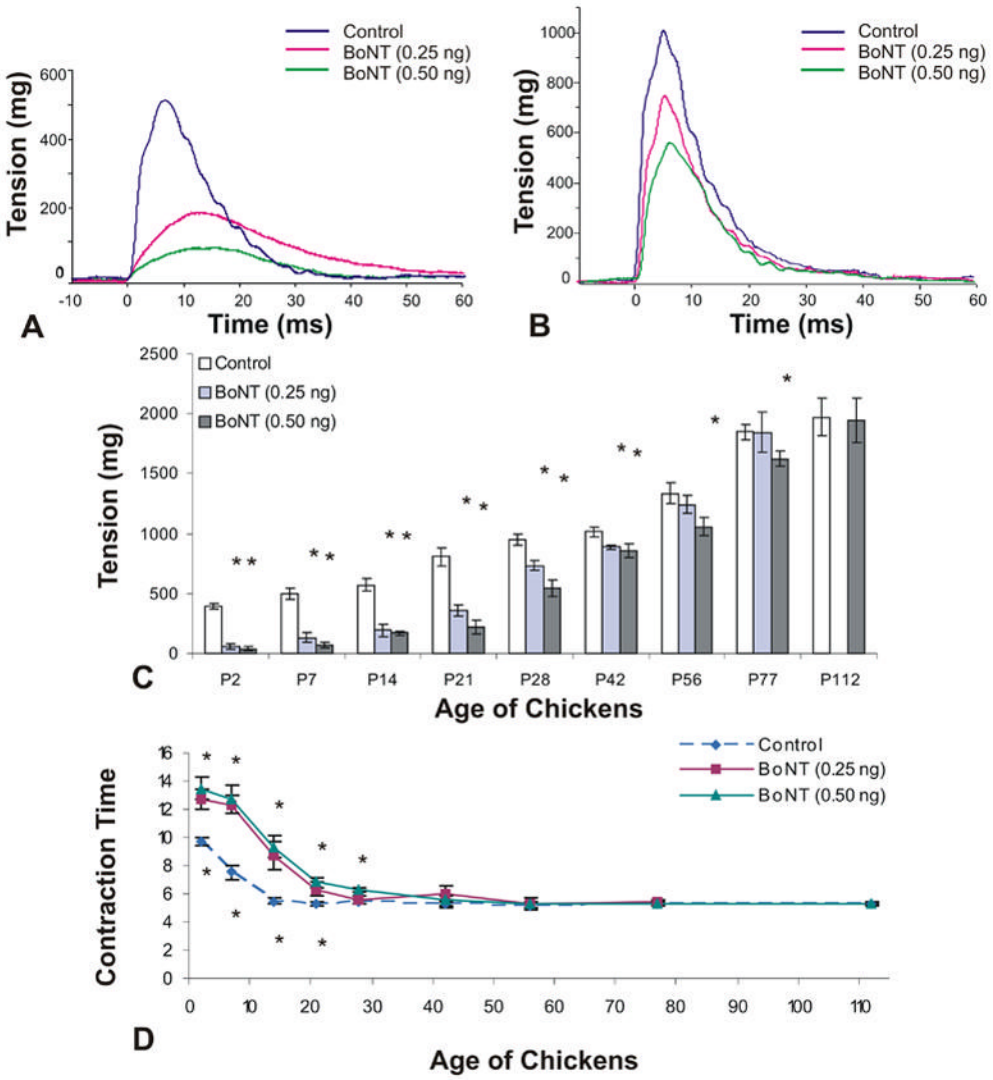

Figure 2.

Isometric twitch tension and contraction time measurements of chick superior oblique muscle. A single dose of botulinum neurotoxin (BoNT, 0.25 ng or 0.50 ng) was injected at day of hatching (P0) and contractile force was measured between the ages of P2 and P112. A and B, Examples of twitch tension in control and BoNT-injected animals examined at post-hatch day 7 (P7) and P28. C and D, Time course of twitch tension and contraction time from P2-P112. Statistically significant differences ($p<0.05$) between control and treated muscles are indicated with an asterisk (C,D). For panel D, asterisks for the higher dose are shown above, and for the lower dose below the data points.

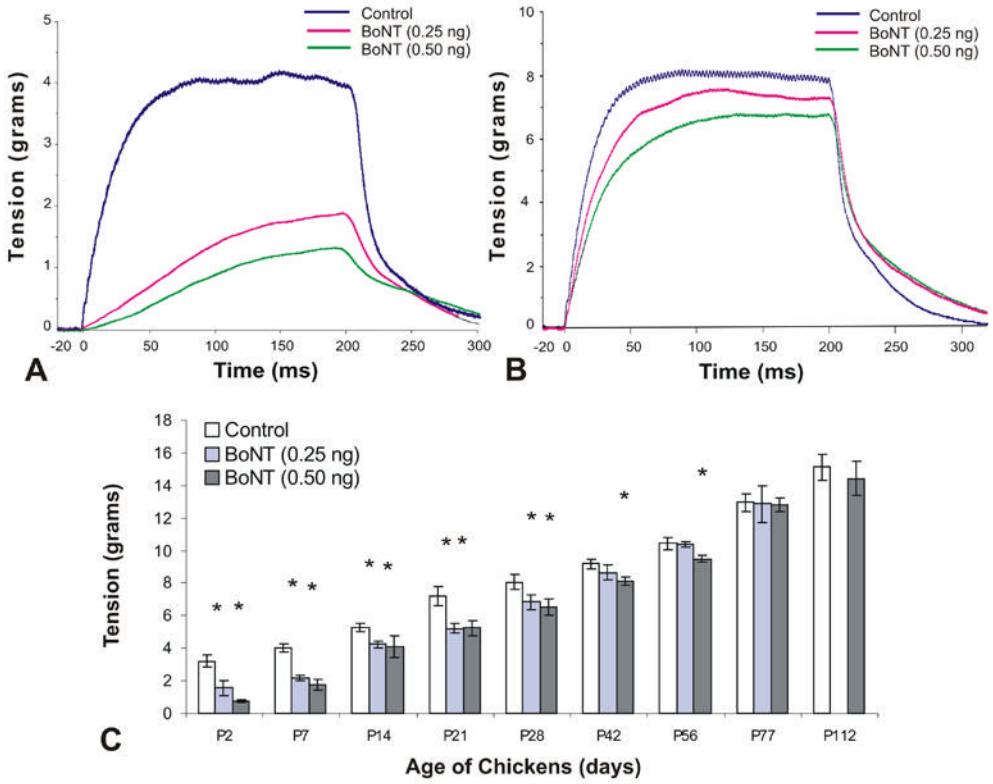

Figure 3.

Isometric tetanic tension measurements of chick superior oblique muscle. A single dose of botulinum neurotoxin (BoNT, 0.25 ng or 0.50 ng) was injected at day of hatching (P0) and contractile force was measured between the ages of P2 and P112. A and B, Examples of tetanic tension in control and BoNT-injected animals examined at post-hatch day 7 (P7) and P28. C, Time course of tetanic tension from P2 to P112. Statistically significant differences ($p<0.05$) between control and treated muscles are indicated with an asterisk (C).

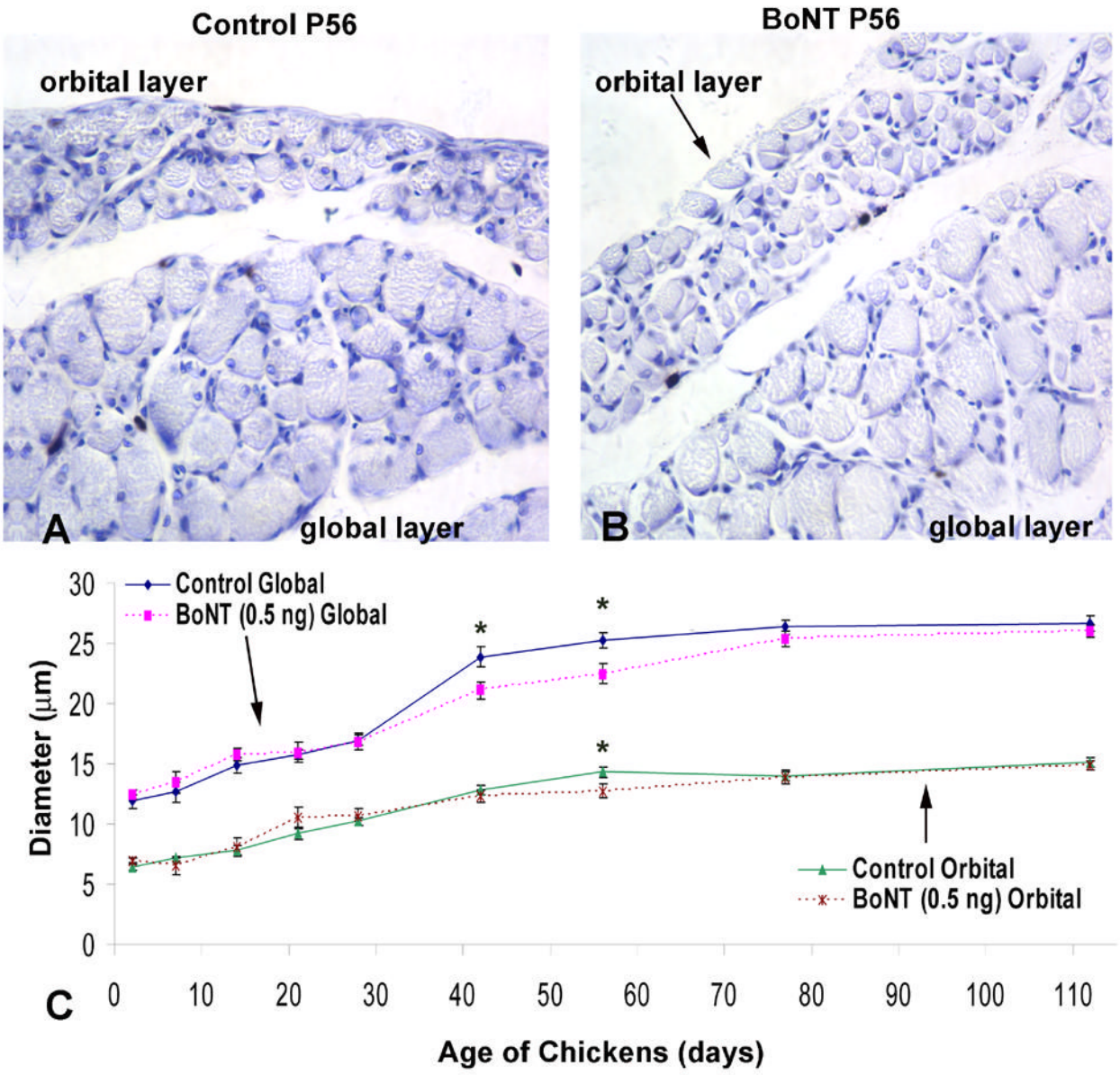

Figure 4.

Myofiber cross sectional diameter of the orbital and global layers of chick superior oblique muscle. A single dose of botulinum neurotoxin (BoNT, 0.50 ng) was injected into the superior oblique muscle at day of hatching (P0) and tissues were collected at ages P2, P7, P14, P21, P28, P42, P56, P77 and P112. A and B, Examples of cross sections showing myofibers within the orbital and global layers of control and BoNT injected extraocular muscles examined at post-hatch day 56 (P56). C, Time course of changes in myofiber diameter within the orbital and global layers of control and BoNT-injected muscle examined between P2 and P112. BoNT induced a significant, but transient decrease in myofiber diameter within the global layer from P42-P77, and within the orbital layer from P56-P77.

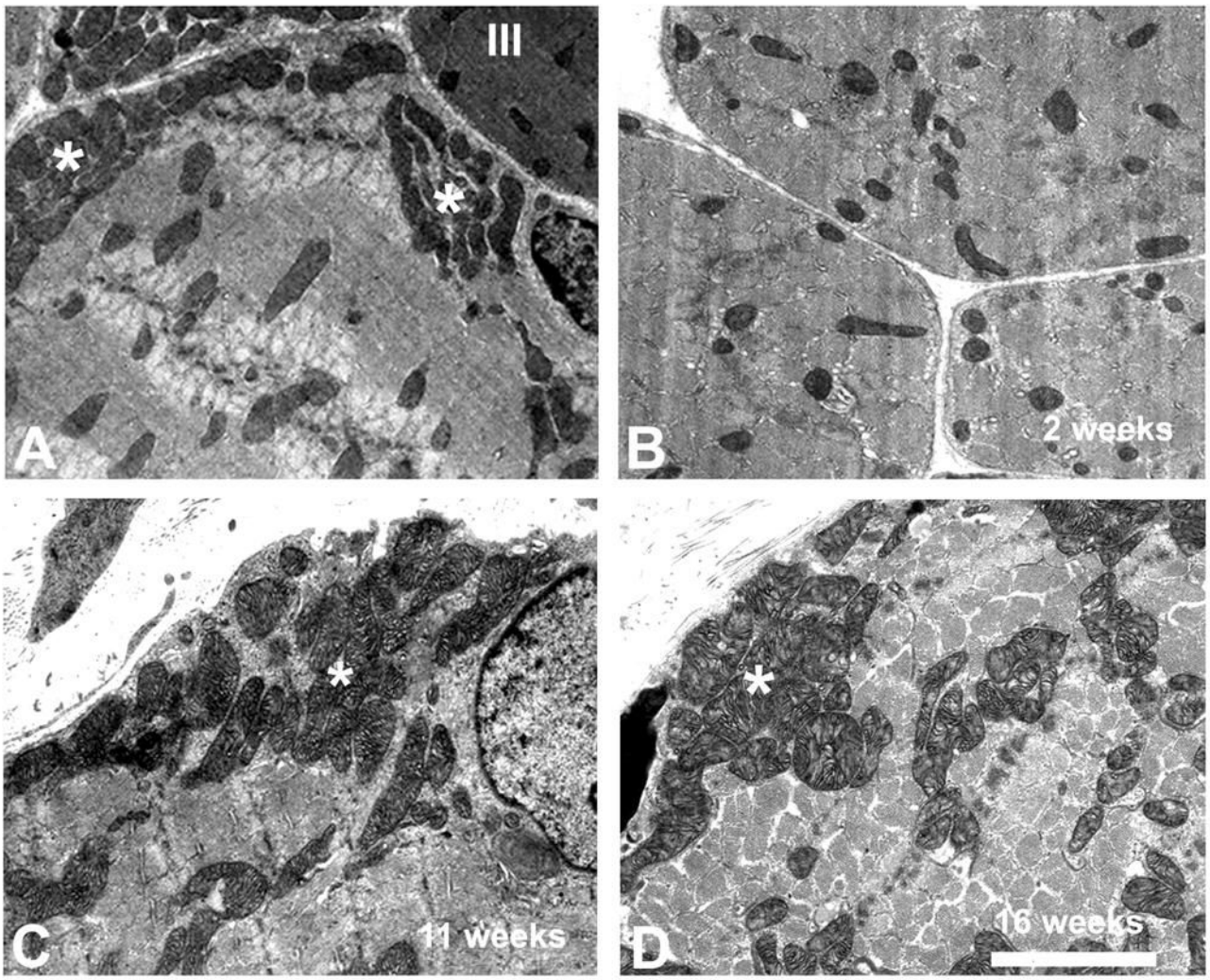

Figure 5.

Ultrastructural morphology and distribution of mitochondria in global layer myofibers of the superior oblique extraocular muscle of chickens with and without treatment of botulinum toxin (BoNT). A, Thin section shows muscle fibers of type-II (pale muscle fibers) from a 2-week old control chick with typical large-sized mitochondria and subsarcolemmal clusters (asterisks). Note the relatively large size and clustering of mitochondria in the type II myofiber. A type III muscle fiber (dark) with typical smaller mitochondria is visible in the upper right corner (III). B, Myofiber from a BoNT-treated chick at 2 weeks of age. Note the lack of clusters, smaller size and dispersed distribution of mitochondria in a type II myofiber. C, Myofiber type II in a control chicken at 11 weeks of age. Note the clustering (asterisk) and the relatively large size of mitochondria. D, Myofiber type II of a BoNT-treated chicken at 16 weeks of age. Note the increased size of mitochondria, and the recovery of clusters (asterisk). Scale bar (same for A–D) = 2.5 μm.

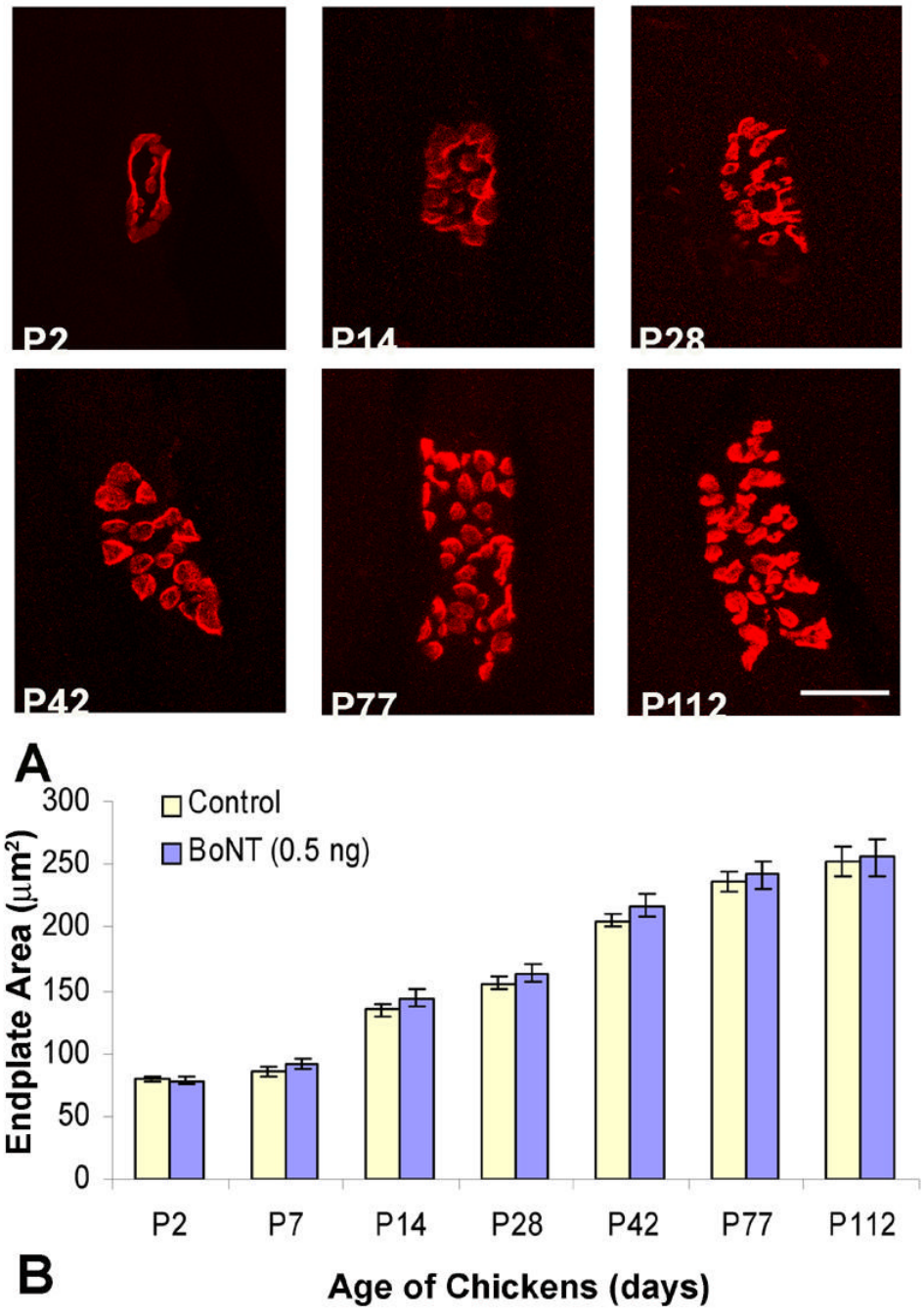

Figure 6.

Images of motor endplates and area measurements in chick superior oblique muscles. A single dose of botulinum neurotoxin (BoNT, 0.50 ng) was injected at day of hatching (P0) and tissues were collected between the ages of P2 and P112. A, Confocal images of motor endplates of control animals from post-hatch day 2 (P2) to post-hatch day 112 (P112). Images from experimental endplates are not shown, because they were indistinguishable to controls (B). Acetylcholine receptors of motor endplates (red) were labeled with rhodamine-conjugated α-bungarotoxin (Rh-αBTX). Scale bar, 10 μm. B, Time course of increases in motor endplate area from P2 to P112. The motor endplates of both control and BoNT treatment groups

increased as the chicks matured, but did not show significant differences between treatment groups.

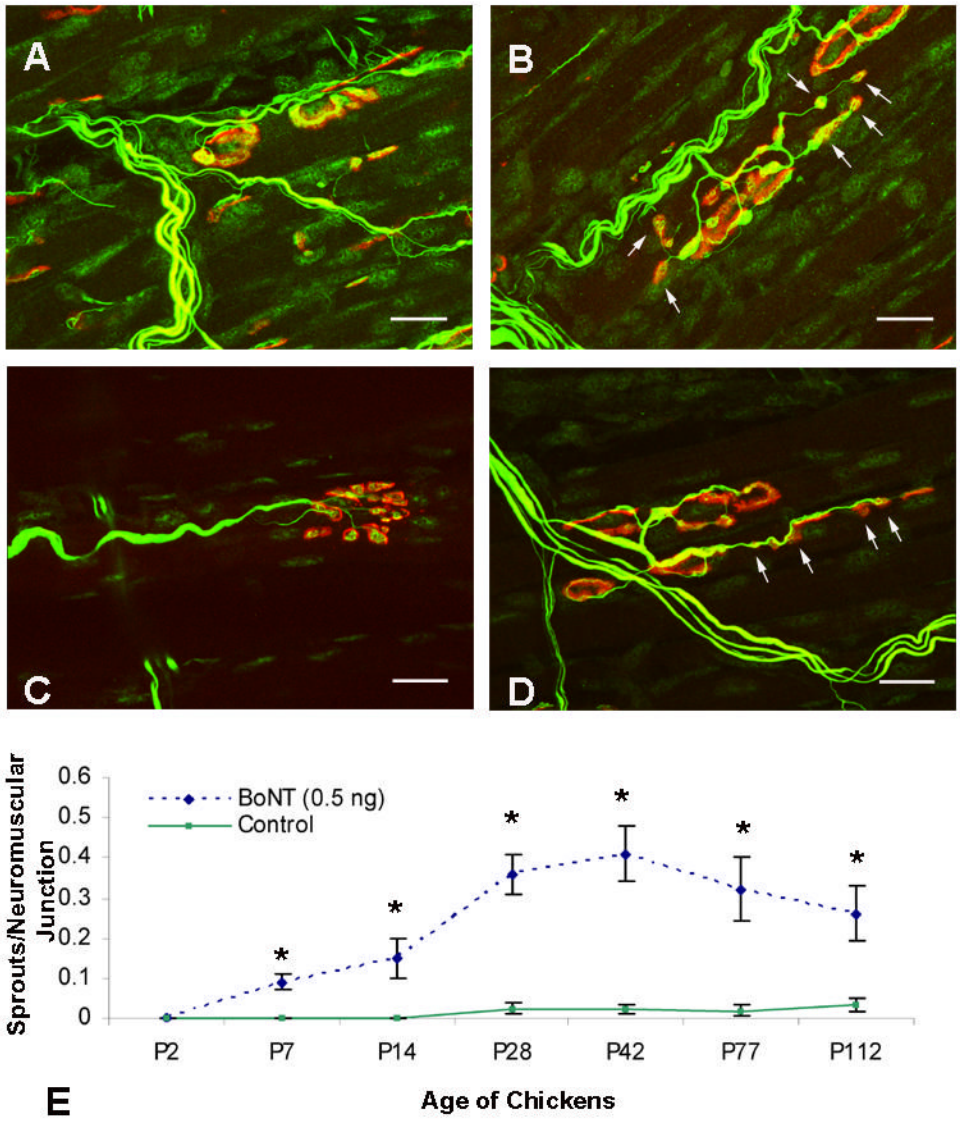

Figure 7.

Confocal images of control and botulinum neurotoxin (BoNT)-treated motor endplates (red) and nerve terminals (green) in chick superior oblique muscle. Control (A, C) muscles exhibited nerve terminal branches that innervated a single motor endplate, whereas BoNT-treated (B, D) muscles displayed sprouts that were often colocalized with acetylcholine receptor clusters (arrows). All scale bars = 10 μm. Treatment with BoNT resulted in the average number of sprouts per neuromuscular junction to increase from P2 to P42 and then decrease between P42 and P112 (E). Statistically significant differences ($p<0.05$) between control and treated muscles are indicated with an asterisk (E). Axons and nerve terminals (both green) were labeled with anti-neurofilament antibodies and anti-SV2 antibodies, respectively, and acetylcholine receptors of motor endplates (red) were labeled with rhodamine-conjugated α-bungarotoxin. Values are the mean ± SEM of measurements from 20 endplates in at least 3 chickens for each time point.

Table 1

Area, diameter and perimeter of mitochondria in myofibers of types I, II, and IV in superior oblique muscles of control (Con) chickens and after injection of botulinum neurotoxin (BoNT). Numbers in bold are statistically significant between controls and BoNT ($p<0.001$).

Layer	**Orbital**								**Global**							
Age	**2 week**		**11 week**		**16 week**		**22 week**		**2 week**		**11 week**		**16 week**		**22 week**	
	Con	**BoNT**	**Con**	**BoNT**	**Con**	**BoNT**	**Con**	**BoNT**	**Con**	**BoNT**	**Con**	**BoNT**	**Con**	**BoNT**	**Con**	**BoNT**
Area [μm^2] ± SEM	**0.035** ± 0.002	**0.010** ± 0.0004	**0.044** ± 0.002	**0.036** ± 0.001	0.135 ± 0.003	0.124 ± 0.005	0.106 ± 0.006	0.106 0.006	**0.039** ± 0.001	**0.012** ± 0.0005	0.047 ± 0.002	0.042 ± 0.002	0.141 ± 0.006	0.140 ± 0.006	0.226 ± 0.014	0.223 ± 0.010
Diameter [μm] ± SEM	**0.20** ± 0.005	**0.10** ± 0.002	**0.22** ± 0.005	**0.20** ± 0.004	0.39 ± 0.004	0.39 ± 0.007	0.35 ± 0.006	0.36 ± 0.006	**0.21** ± 0.004	**0.11** ± 0.002	0.23 ± 0.007	0.22 ± 0.005	0.41 ± 0.009	0.41 ± 0.009	0.51 ± 0.016	0.52 ± 0.011
Perimeter [μm] ± SEM	**0.76** ± 0.02	**0.41** ± 0.01	0.86 ± 0.02	0.84 ± 0.02	1.58 ± 0.03	1.56 ± 0.03	1.29 ± 0.024	1.33 ± 0.023	**0.82** ± 0.02	**0.43** ± 0.01	0.92 ± 0.03	0.90 ± 0.03	1.64 ± 0.04	1.64 ± 0.04	1.95 ± 0.068	1.94 ± 0.045
n	161	252	186	287	95	95	76	94	172	290	122	105	95	95	302	249

Table 2

Area, diameter and perimeter of mitochondria in myofibers of type III in superior oblique muscles of control (Con) chickens and after injection of botulinum neurotoxin (BoNT). Numbers in bold are statistically significant between controls and BoNT ($p<0.001$).

Layer	**Orbital**								**Global**							
Age	**2 week**		**11 week**		**16 week**		**22 week**		**2 week**		**11 week**		**16 week**		**22 week**	
	Con	**BoNT**	**Con**	**BoNT**	**Con**	**BoNT**	**Con**	**BoNT**	**Con**	**BoNT**	**Con**	**BoNT**	**Con**	**BoNT**	**Con**	**BoNT**
Area [μm^2] ± SEM	**0.009** ± 0.0005	**0.006** ± 0.0002	0.011 ± 0.001	0.014 ± 0.001	0.025 ± 0.0007	0.025 ± 0.001	0.035 ± 0.002	0.031 ± 0.001	**0.021** ± 0.002	**0.007** ± 0.0005	**0.019** ± 0.001	**0.011** ± 0.0005	0.025 ± 0.001	0.024 ± 0.001	0.047 ± 0.002	0.043 ± 0.002
Diameter [μm] ± SEM	**0.10** ± 0.002	**0.08** ± 0.001	0.11 ± 0.005	0.13 ± 0.005	0.17 ± 0.002	0.17 ± 0.004	0.20 ± 0.006	0.19 ± 0.005	**0.14** ± 0.005	**0.09** ± 0.003	**0.14** ± 0.004	**0.11** ± 0.002	0.17 ± 0.004	0.17 ± 0.003	0.22 ± 0.005	0.22 0.005
Perimeter [μm] ± SEM	**0.41** ± 0.01	**0.33** ± 0.007	**0.45** ± 0.02	**0.55** ± 0.03	0.71 ± 0.01	0.70 ± 0.01	0.80 ± 0.03	0.75 ± 0.024	**0.58** ± 0.02	**0.37** ± 0.01	**0.61** ± 0.02	**0.46** ± 0.01	0.72 ± 0.02	0.71 ± 0.02	0.81 ± 0.019	0.84 ± 0.021
n	110	265	50	49	74	65	107	84	186	121	179	216	81	95	74	110

Table 3

Fractional area [%] of mitochondria in myofibers of types I, II, III and IV in superior oblique muscles of control (Con) chickens and after injection of botulinum neurotoxin (BoNT). Numbers in bold indicate statistically significant differences between control and BoNT ($p<0.001$). Values are presented separately for mitochondria "clustered" in subsarcolemmal regions (SS) and "non-clustered" in the interfibrillar myofiber regions (IF). For each value (mean ±SEM), 10–20 view fields were sampled randomly at 25,000–35,000x magnification.

Layer:	**Orbital**								**Global**							
Age:	**2 week**		**11 week**		**16 week**		**22 week**		**2 week**		**11 week**		**16 week**		**22 week**	
	Con	**BoNT**	**Con**	**BoNT**	**Con**	**BoNT**	**Con**	**BoNT**	**Con**	**BoNT**	**Con**	**BoNT**	**Con**	**BoNT**	**Con**	**BoNT**
Fiber Type:																
I (SS)	**44.5**	**0** ± 0	**48.6**	**34.1**	39.7	39.4	30.0	38.9	**42.4**	**0** ± 0	**46.1**	**32.8**	47.3	44.7	44.3	42.8
± SEM	± 2.6		± 3.0	± 2.2	± 2.1	± 2.1	± 2.5	± 4.1	± 6.6		± 4.0	± 3.0	± 1.9	± 2.9	± 5.3	± 3.7
I (IF)	**12.8**	**4.2** ± 0.8	15.7	15.0	28.9	25.8	14.8	15.9	**15.3**	**4.8** ± 1.0	21.3	15.0	30.0	24.8	20.7	20.4
± SEM	± 1.6		± 1.3	± 1.7	± 1.5	± 1.1	± 1.4	± 4.7	± 1.5		± 2.9	± 1.6	± 1.75	± 2.9	± 2.3	± 4.0
II (SS)	**40.6**	**0** ± 0	35.6	27.1	30.9	28.6	28.2	35.4	**33.2**	**0** ± 0	34.1	28.4	34.6	34.3	35.4	36.7
± SEM	± 5.7		± 2.7	± 3.8	± 1.1	± 3.4	± 3.9	± 7.3	± 4.1		± 2.0	± 3.9	± 2.5	± 3.3	± 7.7	± 5.1
II (IF)	**13.8**	**4.5** ± 1.2	15.5	13.8	**23.3**	**16.4**	19.7	23.9	**10.9**	**6.7** ± 0.3	17.1	11.9	21.7	19.6	17.8	17.1
± SEM	± 1.7		± 1.4	± 2.2	± 0.8	± 1.1	± 1.9	± 5.8	± 1.6		± 2.4	± 0.7	± 1.3	± 1.1	± 2.3	± 3.4
III (IF)	**2.9**	**1.1** ± 0.3	6.2	3.2 ± 0.6	7.9	6.8 ± 0.9	7.6	5.3 ± 1.3	**8.3**	**4.0** ± 0.3	4.8	4.1 ± 0.5	5.7 ± 0.6	5.6 ± 0.7	5.6	4.8 ± 1.3
± SEM	± 0.6		± 1.4		± 1.0		± 0.9		± 0.8		± 0.7				± 1.4	
IV (SS)	**36.9**	**0** ± 0	30.5	24.8	33.6	31.0	35.7	34.2	**34.7**	**0** ± 0	**43.8**	**29.0**	22.4	21.7	24.1	23.5
± SEM	± 2.0		± 2.6	± 2.2	± 4.2	± 4.2	± 0.4	± 0.8	± 4.9		± 5.6	± 4.7	± 3.5	± 2.8	± 0.4	± 4.4
IV (IF)	**15.2**	**4.1** ± 1.0	17.1	13.4	13.4	13.6	19.1	20.7	**14.5**	**4.1** ± 0.5	**17.9**	**11.7**	7.1 ± 0.9	6.1 ± 1.0	14.9	10.7
± SEM	± 1.3		± 1.8	± 1.7	± 1.3	± 1.9	± 2.4	± 3.7	± 1.8		± 1.9	± 1.0			± 2.0	± 4.1